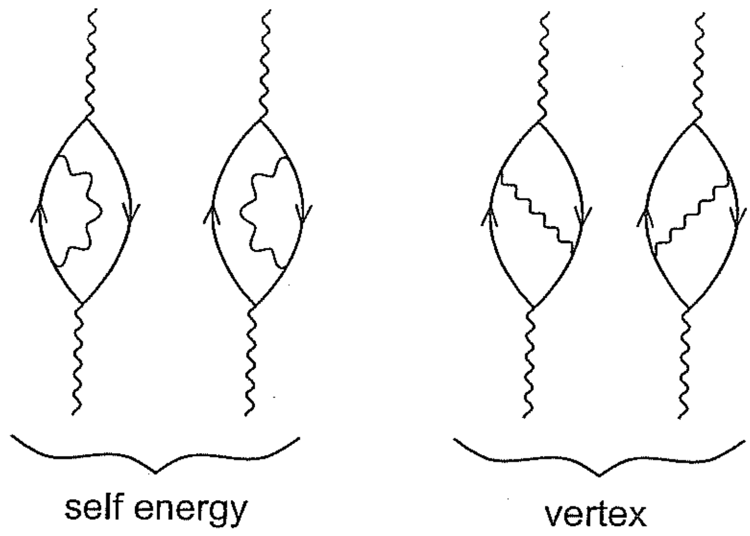


Figure 6.C.3: Lowest order diagrams which dress collective nuclear vibrations and GR.

words, one can take care of the position indeterminacy of a quantal particle (electron) accepting the possibility to observe it through specific measurements which unavoidably create different particles, each of them identical to the original one, but with different positions, to keep track of conserved quantum numbers, these particles are to be accompanied by an equal number of antiparticles (positrons).

Similar results can be obtained by considering vacuum fluctuations (ZPF), and forcing them to become real through e.g. the Pauli principle (Pauli, 1947), as Fig. observed in the Lamb shift (Fig. 6.C.2; cf. also 6.D).

In the nuclear case the medium can, due to spatial quantization typical of Finite Many–Body Systems (FMBS), propagate information with varied frequency. Typically, few MeV (low–lying collective vibrations) and tens of MeV (giant resonances), leading to a rich number of CO and PO processes. This is in keeping with the fact that the intermediate boson (photon QED, vibrations of nuclear medium) propagates in a medium which is not isotropic, thus undergoing fragmentation ~~of~~ , let alone when the GR is based on the ground state the associated strength (inhomogeneous damping). To make even richer the nuclear scenario, collisional damping plays also a role in the strength function of GR. Nonetheless, the associated widths (lifetimes) are controlled by the coupling to doorway states, even at nuclear temperatures of 1–2 MeV (Fig. 6.C.3; cf. Bortignon et al. (1998) and refs. therein). The strong cancellation found between self–energy and vertex correction diagrams, testify to the collectivity of nuclear vibrations, and reminds of Furry's theorem (no coupling between one– and two–photon states). Summing up, nothing is really free in the quantal world. Selected measurements carried out with specific probes, can make virtual processes become real, and shed light on the variety of these processes leading to ~~effective fields~~

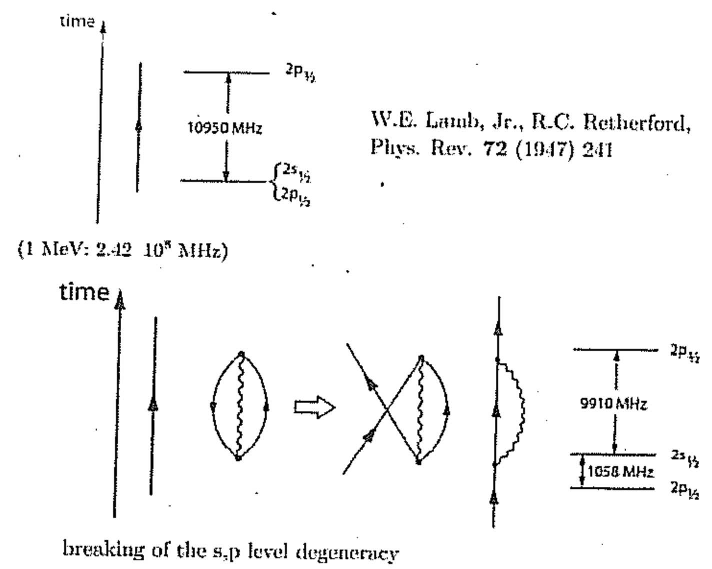


Figure 6.D.1: Schematic representation of the processes associated with the Lamb shift.

renormalized, elementary modes of nuclear excitation

(dressed fermions and bosons).

## Appendix 6.D The Lamb Shift

In Fig. 6.D.1 we display a schematic summary of the electron–photon processes, associated with Pauli principle corrections, leading to the splitting of the lowest $s, p$ states of the hydrogen atom known as the Lamb shift.

In the upper part of the figure the predicted position of the electronic single–particle levels of the hydrogen atom as resulting from the solution of the Scrödinger equation (Coulomb field). In the lowest part of the figure one displays the electron of an hydrogen atom (upwards going arrowed line) in presence of vacuum ZPF (electron–positron pair plus photon, oyster–like diagram) (within this scenario we refer to App. 6.C concerning to the central role ZPF of the vacuum and the concept of antiparticle (hole) has in the description of physical, dressed observable states of quantal many–body systems). Because the associate electron virtually occupies states already occupied by the hydrogen's electron, thus violating Pauli principle, one has to antisymmetrize the corresponding two–electron state. Such process gives rise to the exchange of the corresponding fermionic lines and thus to CO–like diagrams as well as, through time ordering, to PO–like diagrams. The results provide a quantitative account of the experimental findings.

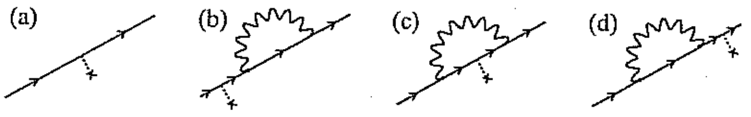


Figure 6.E.1: Self energy (effective–mass–like) processes. The result of the probing with an external field (dotted line started with a cross, observer) of the properties (mass, single–particle energy, etc) of a fermion (e.g. an electron or a nucleon, arrowed line) dressed through the coupling of (quasi) bosons (photons or collective vibrations, wavy line), corresponds to the modulus squared of the sum of the amplitudes associated with each of the four diagrams (a)–(d) (cf. (Feynman, 1975)). A concrete embodiment of the above parlance is provided by the process $^{1}H(^{11}Li,^{9}Li)^{3}H$ (cf. Figs. 6.1.4 and 6.1.5).

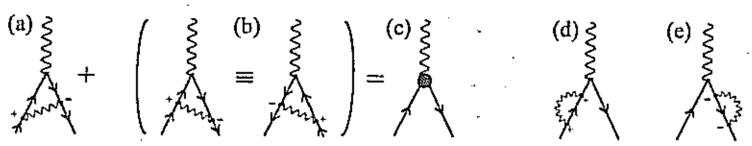


Figure 6.E.2: Vertex corrections. These are triple–interaction vertex diagrams in which none of the incoming lines can be detached from either of the other two by cutting one line. Migdal's (Migdal, 1958) theorem states that, for phonons and electrons (Bardeen–Pines (Bardeen and Pines, 1955)–Frölich (Frohlich, 1952) mechanism to break gauge invariance), vertex corrections can be neglected, but usually they are not negligible, in any case not in nuclei (cancellation) (cf. e.g. Anderson (1984)). The solid grey circle in (c) represents the effective, renormalized vertex.

ö

Frölich

The distorted wave programs numerically evaluate the quantity $B^l_{m_l}(\theta)$, using for the wave functions $\chi^{(-)}$ and $\chi^{(+)}$ the solution of the optical potentials that fit the elastic scattering, i.e.

E

$$(-\nabla^2 + \bar{U} - k^2)\chi = 0, \qquad (6.F.14)$$

E

(see eq. (4.2.11)). Note that if the target nucleus is even, $I_A = 0$, $l = I_{A+1}$. That is, only one $l$ value contributes in eq. (6.F.8), and the angular distribution is uniquely given by $\sum_m |B^l_m|^2$. The $l$-dependence of the angular distributions helps to identify $l = I_{A+1}$. The factor $S_l$ needed to normalize the calculated function to the data yields (assuming a good fit to the angular distribution), is known in the literature as the spectroscopic factor. It was assumed in the early stages of studies of nuclear structure with one–particle transfer reactions not only that it could be defined, but also that it contained all the nuclear structure information (aside from that associated with the angular distribution) which could be extracted from ~~single–particle~~ transfer. In other words, that it was the bridge directly ~~connecting~~ theory with experiment. Because nucleons are never bare, but ~~are~~ dressed by the coupling to collective modes as previously discussed in this Chapter, the spectroscopic factor approximation is at best a helpful tool to get order of magnitude information from one–particle transfer data.

c lower case

There is a fundamental problem which makes the handling of integrals like that of (6.F.9) difficult to handle, if not numerically at least conceptually. This difficulty is connected with the so called recoil effect[3], namely the fact that the center of mass of the two interacting particles in entrance ($\mathbf{r}_\alpha : \alpha = a + A$) and exit ($\mathbf{r}_\beta : \beta = b + B$) channels is different. This is at variance with what one is accustomed to deal with in nuclear structure calculations, in which the Hartree potential depends on a single coordinate, as well as in the case of elastic and inelastic reactions, situations in which $\mathbf{r}_\alpha = \mathbf{r}_\beta$. When $\mathbf{r}_\alpha \neq \mathbf{r}_\beta$ we enter a rather more complex many–body problem, in particular if continuum states are to be considered, than nuclear structure practitioners were accustomed to.

Of notice that similar difficulties have been faced in connection with the non–local Fock (exchange) potential. As a rule, the corresponding (HF) mean field equations are rendered local making use of the $k$–mass approximation or within the framework of Local Density Functional Theory (DFT), in particular with the help of the Kohn–Sham equations (see e.g. C. Mahaux et al. (1985), Broglia et al. (2004) and refs. therein; cf. also App. 6.A). Although much of the work in this field is connected with the correlation potential (interweaving of single–particle and collective motion), an important fraction is connected with the exchange potential.

In any case, and returning to the subject of the present appendix, it is always useful to be able to introduce approximations which can help the physics which is at the basis of the phenomenon under discussion (single–particle motion) emerge

[3] While this effect could be treated in a cavalier fashion in the case of light ion reactions ($m_a/m_A \ll 1$), this was not possible in the case of heavy ion reactions, as the change in momenta involved was always sizeable (cf. Broglia and Winther (2004) and refs. therein).

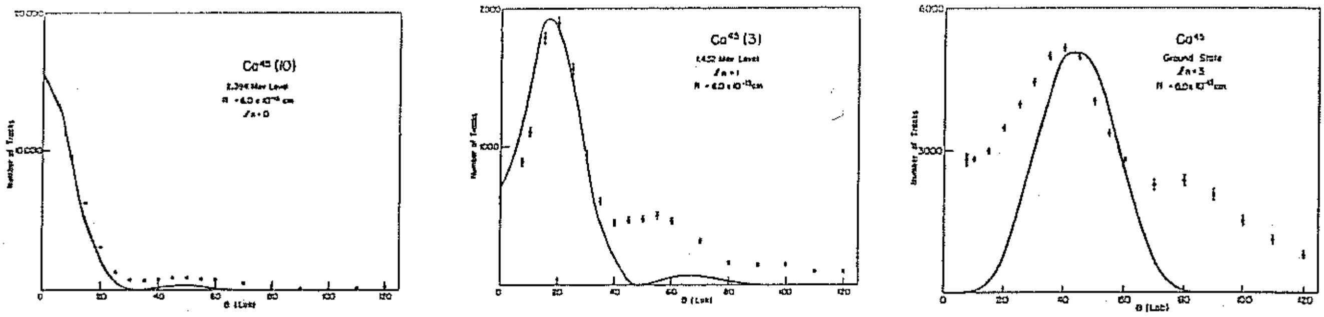

Figure 6.F.2: Plane wave approximation analysis of three $^{44}$Ca(d,p)$^{45}$Ca differential cross sections leading to the ground state ($l$ = 3) and to the 1.9 MeV state ($l$ = 1) and 2.4 MeV ($l$ = 0) excited states, i.e. $f_{9/2}$, $p_{1/2}$ and $s_{1/2}$ states (Cobb and Guthe, 1957).

Thus, the angular distribution is given by the integral $\left|\int r^2 dr\, j_l(qr) u_l(r)\right|^2$. If one assumes that the process takes place mostly on the surface, the angular distribution will be given by $|j_l(qR_0)|^2$, where $R_0$ is the nuclear radius.

We then have

$$\begin{aligned} q^2 &= k_d^2 + k_p^2 - 2k_d k_p \cos(\theta) \\ &= (k_d^2 + k_p^2 - 2k_d k_p) + 2k_d k_p (1 - \cos(\theta)) \\ &= (k_d - k_p)^2 + 4k_d k_p \,(\sin(\theta/2))^2 \\ &\approx 4k_d k_p \,(\sin(\theta/2))^2 \,, \end{aligned} \tag{6.F.22}$$

since $k_d \approx k_p$ for stripping reactions at typical energies. Thus the angular distribution has a diffraction-like structure given by

$$|j_l(qR_0)|^2 = j_l^2(2R_0\sqrt{k_d k_p}\sin(\theta/2)). \tag{6.F.23}$$

The function $j_l(x)$ has its first maximum at $x = l$, i.e. where

$$\sin(\theta/2) = \frac{l}{2R_0 k}, \qquad (k_p \approx k_d = k), \tag{6.F.24}$$

Examples of the above relation are provided in Fig. 6.F.2.

## Appendix 6.G One–particle knockout within DWBA

### 6.G.1 Spinless particles

We are going to consider the reaction $A + a \to a + b + c$, in which the cluster $b$ is knocked out from the nucleus $A(= c + b)$. Cluster $b$ is thus initially bound, while the final states of $a, b$ and the initial state of $a$ are all in the continuum, and final channel wavefunction describing the relative motion of $b$ and $c$, as defined by the complex optical potential $U(r_{bc})$).

**Recoupling of angular momenta**

One now proceeds to the evaluation of the 6–dimensional integral

$$\begin{aligned}
&\frac{64\pi^3}{k_a k'_a k'_b} \int d\mathbf{r}_{aA} d\mathbf{r}_{bc} u_{l_b}(r_{cb}) v(r_{ab}) \sum_{l_a, l'_a, l'_b} \sqrt{(2l_a+1)(2l'_a+1)(2l'_b+1)} \\
&\quad \times e^{i(\sigma^{l_a} + \sigma^{l'_a} + \sigma^{l'_b})} \frac{F_{l_a}(r_{aA}) F_{l'_a}(r_{ac}) F_{l'_b}(r_{bc})}{r_{ac} r_{aA} r_{bc}} \\
&\quad \times \left[Y^{l_a}(\hat{\mathbf{r}}_{aA}) Y^{l_a}(\hat{\mathbf{k}}_a)\right]_0^0 \left[Y^{l'_a}(\hat{\mathbf{r}}_{ac}) Y^{l'_a}(\hat{\mathbf{k}}'_a)\right]_0^0 \left[Y^{l'_b}(\hat{\mathbf{r}}_{bc}) Y^{l'_b}(\hat{\mathbf{k}}'_b)\right]_0^0 Y^{l_b}_{m_b}(\hat{\mathbf{r}}_{bc}),
\end{aligned} \tag{6.G.9}$$

an expression which explicitly depends on the asymptotic kinetic energies and scattering angles $(\hat{\mathbf{k}}_a, \hat{\mathbf{k}}'_a, \hat{\mathbf{k}}'_b)$ of $a, b$ as determined by $k_a, k'_a, k'_b$ and $\hat{\mathbf{k}}_a, \hat{\mathbf{k}}'_a, \hat{\mathbf{k}}'_b$ respectively. In what follows we will take advantage of the partial wave expansion to reduce the dimensionality of the integral from 6 to 3. A possible strategy to follow is that of recoupling together all the terms that depend on the integration variables to a global angular momentum and retain only the term coupled to 0 as the only one surviving the integration. Let us start to separately couple the terms corresponding to particles $a$ and $b$. For particle $a$ we write

$$\begin{aligned}
&\left[Y^{l_a}(\hat{\mathbf{r}}_{aA}) Y^{l_a}(\hat{\mathbf{k}}_a)\right]_0^0 \left[Y^{l'_a}(\hat{\mathbf{r}}_{ac}) Y^{l'_a}(\hat{\mathbf{k}}'_a)\right]_0^0 = \sum_K ((l_a l_a)_0 (l'_a l'_a)_0 | (l_a l'_a)_K (l_a l'_a)_K)_0 \\
&\qquad \times \left\{\left[Y^{l_a}(\hat{\mathbf{r}}_{aA}) Y^{l'_a}(\hat{\mathbf{r}}_{ac})\right]^K \left[Y^{l_a}(\hat{\mathbf{k}}_a) Y^{l'_a}(\hat{\mathbf{k}}'_a)\right]^K\right\}_0^0 .
\end{aligned} \tag{6.G.10}$$

We can now evaluate the 9j symbol,

9j-symbol

$$((l_a l_a)_0 (l'_a l'_a)_0 | (l_a l'_a)_K (l_a l'_a)_K)_0 = \sqrt{\frac{2K+1}{(2l'_a+1)(2l_a+1)}}, \tag{6.G.11}$$

and expand the coupling,

$$\begin{aligned}
&\left\{\left[Y^{l_a}(\hat{\mathbf{r}}_{aA}) Y^{l'_a}(\hat{\mathbf{r}}_{ac})\right]^K \left[Y^{l_a}(\hat{\mathbf{k}}_a) Y^{l'_a}(\hat{\mathbf{k}}'_a)\right]^K\right\}_0^0 = \sum_M \langle K\ K\ M\ -M | 0\ 0 \rangle \\
&\times \left[Y^{l_a}(\hat{\mathbf{r}}_{aA}) Y^{l'_a}(\hat{\mathbf{r}}_{ac})\right]_M^K \left[Y^{l_a}(\hat{\mathbf{k}}_a) Y^{l'_a}(\hat{\mathbf{k}}'_a)\right]_{-M}^K = \sum_M \frac{(-1)^{K+M}}{\sqrt{2K+1}} \\
&\times \left[Y^{l_a}(\hat{\mathbf{r}}_{aA}) Y^{l'_a}(\hat{\mathbf{r}}_{ac})\right]_M^K \left[Y^{l_a}(\hat{\mathbf{k}}_a) Y^{l'_a}(\hat{\mathbf{k}}'_a)\right]_{-M}^K .
\end{aligned} \tag{6.G.12}$$

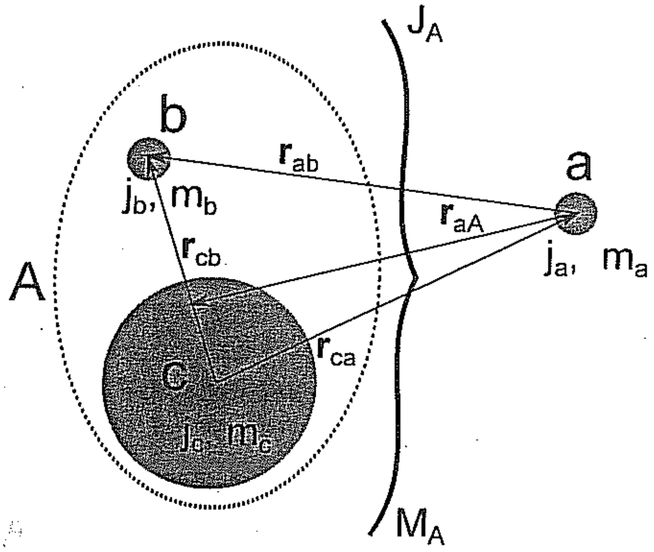


Figure 6.G.3: ~~Now~~ all three clusters $a, b, c$ have definite spins and projections. The nucleus $A$ is coupled to total spin $J_A, M_A$.

In the present case

**Zero range approximation.**

The zero range approximation consists in taking $v(r_{ab}) = D_0\delta(r_{ab})$. Then, (see (6.G.21))

$$\mathbf{r}_{aA} = \frac{c}{A}\mathbf{r}_{bc}, \qquad \mathbf{r}_{ac} = \mathbf{r}_{bc}. \tag{6.G.52}$$

The angular dependence of the integral can be readily evaluated. From (7.K.20), noting that $\hat{\mathbf{r}}_{aA} = \hat{\mathbf{r}}_{ac} = \hat{\mathbf{r}}_{bc} \equiv \hat{\mathbf{r}}$,

$$\begin{aligned}\left[Y^{l_a}(\hat{\mathbf{r}})Y^{l'_a}(\hat{\mathbf{r}})\right]^K_M \left[Y^{l_b}(\hat{\mathbf{r}})Y^{l'_b}(\hat{\mathbf{r}})\right]^K_{-M} = \\ \frac{(-1)^{K-M}}{\sqrt{2K+1}}\left\{\left[Y^{l_a}(\hat{\mathbf{r}})Y^{l'_a}(\hat{\mathbf{r}})\right]^K \left[Y^{l_b}(\hat{\mathbf{r}})Y^{l'_b}(\hat{\mathbf{r}})\right]^K\right\}^0_0.\end{aligned} \tag{6.G.53}$$

We can as before evaluate this expression in the configuration shown in Fig. 6.G.2 ($\hat{\mathbf{r}} = \hat{z}$), but now the multiplicative factor is $4\pi$. The corresponding contribution to the integral is

$$\frac{(-1)^K}{4\pi(2K+1)}\langle l_a\ 0\ l'_a\ 0|K\ 0\rangle \sqrt{(2l_a+1)(2l'_a+1)(2l_b+1)(2l'_b+1)}, \tag{6.G.54}$$

and

$$\begin{aligned}T^{m'_a,m'_b}_{m_a,m_b}(\mathbf{k}'_a, \mathbf{k}'_b) = \frac{16\pi^2}{k_a k'_a k'_b}\frac{c}{A}D_0 T_\sigma \sum_{l_a,j_a}\sum_{l'_a,j'_a}\sum_{l'_b,j'_b}\sum_{K,M} e^{i(\sigma^{l_a}+\sigma^{l'_a}+\sigma^{l'_b})} i^{l_a-l'_a-l'_b}(-1)^{l_a+l'_a+l'_b-j'_a-j'_b} \\ \times \sqrt{(2l_a+1)(2l'_a+1)(2l_b+1)(2l'_b+1)}\,\langle l_a\ 0\ l'_a\ 0|K\ 0\rangle \\ \times \frac{2l_a+1}{2K+1}((l'_a\tfrac{1}{2})_{j'_a}(l_a\tfrac{1}{2})_{j_a}|(l_a l'_a)_K(\tfrac{1}{2}\tfrac{1}{2})_0)_K\,((l'_b\tfrac{1}{2})_{j'_b}(l_b\tfrac{1}{2})_{j_b}|(l_b l'_b)_K(\tfrac{1}{2}\tfrac{1}{2})_0)_K \\ \times \langle l'_a\ m_a - m'_a - M\ 1/2\ m'_a|j'_a\ m_a - M\rangle\langle l'_b\ m_b - m'_b + M\ 1/2\ m'_b|j'_b\ M + m_b\rangle \\ \times \langle l\ 0\ 1/2\ m_a|j\ m_a\rangle Y^{l'_b}_{M+m_b+m'_b}(\hat{\mathbf{k}}'_b)Y^{l'_a}_{m_a+m'_a-M}(\hat{\mathbf{k}}'_a)\mathcal{I}_{ZR}(l_a, l'_a, l'_b, j_a, j'_a, j'_b),\end{aligned} \tag{6.G.55}$$

where now the 1–dimensional integral to solve is

$$\mathcal{I}_{ZR}(l_a, l'_a, l'_b, j_a, j'_a, j'_b) = \int dr u_{l_b}(r)F_{l_a,j_a}(\tfrac{c}{A}r)F_{l'_a,j'_a}(r)F_{l'_b,j'_b}(r)/r. \tag{6.G.56}$$

## 6.G.3 One–particle transfer

It may be interesting to state the expression for the one particle transfer reaction within the same context and using the same elements, in order to better compare these two type of experiments. In particle transfer, the final state of $b$ is a bound

(cf. Fig. 6.G.4)

Gregory OK ?

La Fig. 6.G.4 no viene call, en ningún lugar.

state of the $B(=a+b)$ nucleus, and we can carry on in a similar way as done previously just by substituting the distorted wave (continuum) wave function (6.G.34) with

$$\psi^{l'_b,j'_b*}_{m'_b}(\mathbf{r}_{ab},\sigma_b) = u^*_{l'_b,j'_b}(r_{ab})\left[Y^{l'_b}(\hat{\mathbf{r}}_{ab})\phi^{1/2}(\sigma_b)\right]^{j'_b*}_{m'_b}, \tag{6.G.57}$$

so the transition amplitude is now

$$\begin{aligned}
T^{m'_a,m'_b}_{m_a,m_b}(\mathbf{k}'_a) = \frac{8\pi^{3/2}}{k_a k'_a}&\sum_{\sigma_a,\sigma_b}\sum_{l_a,j_a}\sum_{l'_a,m_{l'_a},j'_a} e^{i(\sigma^{l_a}+\sigma^{l'_a})} i^{l_a-l'_a}(-1)^{l_a+l'_a-j'_a-j'_b}\\
&\times\sqrt{2l_a+1}\,\langle l'_a\ m_{l'_a}\ 1/2\ m'_a|j'_a\ m_{l'_a}+m'_a\rangle\langle l_a\ 0\ 1/2\ m_a|j_a\ m_a\rangle\\
\times Y^{l'_a}_{-m_{l'_a}}(\hat{\mathbf{k}}'_a)\int d\mathbf{r}_{aA}d\mathbf{r}_{bc}&\left[Y^{l'_a}(\hat{\mathbf{r}}_{Bc})\phi^{1/2}(\sigma_a)\right]^{j'_a}_{-m_{l'_a}-m'_a}\left[Y^{l'_b}(\hat{\mathbf{r}}_{ab})\phi^{1/2}(\sigma_b)\right]^{j'_b}_{-m'_b}\\
&\times\frac{F_{l_a,j_a}(r_{aA})F_{l'_a,j'_a}(r_{Bc})}{r_{Bc}r_{aA}}u^*_{l'_b,j'_b}(r_{ab})u_{l_b,j_b}(r_{bc})v(r_{ab})v_\sigma(\sigma_a,\sigma_b)\\
&\qquad\times\left[Y^{l_a}(\hat{\mathbf{r}}_{aA})\phi^{1/2}(\sigma_a)\right]^{j_a}_{m_a}\left[Y^{l_b}(\hat{\mathbf{r}}_{bc})\phi^{1/2}(\sigma_b)\right]^{j_b}_{m_b}.
\end{aligned}\tag{6.G.58}$$

Using (6.G.39), (6.G.40), (7.M.4), and setting $M = m_a - m'_a - m_{l'_a}$

$$\begin{aligned}
T^{m'_a,m'_b}_{m_a,m_b}(\mathbf{k}'_a) = \frac{8\pi^{3/2}}{k_a k'_a}T_\sigma&\sum_{l_a,j_a}\sum_{l'_a,j'_a}\sum_{K,M} e^{i(\sigma^{l_a}+\sigma^{l'_a})} i^{l_a-l'_a}(-1)^{l_a+l'_a-j'_a-j'_b}\\
&\times\left((l'_a\tfrac{1}{2})_{j'_a}(l_a\tfrac{1}{2})_{j_a}|(l_al'_a)_K(\tfrac{1}{2}\tfrac{1}{2})_0\right)_K\left((l'_b\tfrac{1}{2})_{j'_b}(l_b\tfrac{1}{2})_{j_b}|(l_bl'_b)_K(\tfrac{1}{2}\tfrac{1}{2})_0\right)_K\\
&\times\sqrt{2l_a+1}\,\langle l'_a\ m_a-m'_a-M\ 1/2\ m'_a|j'_a\ m_a-M\rangle\langle l_a\ 0\ 1/2\ m_a|j_a\ m_a\rangle\\
\times Y^{l'_a}_{m_a-m'_a-M}(\hat{\mathbf{k}}'_a)\int d\mathbf{r}_{aA}d\mathbf{r}_{bc}&\frac{F_{l_a,j_a}(r_{aA})F_{l'_a,j'_a}(r_{Bc})}{r_{Bc}r_{aA}}u^*_{l'_b,j'_b}(r_{ab})u_{l_b,j_b}(r_{bc})v(r_{ab})\\
&\qquad\times\left[Y^{l_a}(\hat{\mathbf{r}}_{aA})Y^{l'_a}(\hat{\mathbf{r}}_{Bc})\right]^K_M\left[Y^{l_b}(\hat{\mathbf{r}}_{bc})Y^{l'_b}(\hat{\mathbf{r}}_{ab})\right]^K_{-M}.
\end{aligned}\tag{6.G.59}$$

Aside from (6.G.21), we also need

$$\mathbf{r}_{Bc} = \frac{a+B}{B}\mathbf{r}_{aA} + \frac{b}{A}\mathbf{r}_{bc}. \tag{6.G.60}$$

From (6.G.20–6.G.25), one gets

$$\begin{aligned}
T^{m'_a,m'_b}_{m_a,m_b}(\mathbf{k}'_a) = \frac{32\pi^3}{k_a k'_a}T_\sigma&\sum_{l_a,j_a}\sum_{l'_a,j'_a}\sum_{K,M} e^{i(\sigma^{l_a}+\sigma^{l'_a})} i^{l_a-l'_a}(-1)^{l_a+l'_a-j'_a-j'_b}\\
&\times\left((l'_a\tfrac{1}{2})_{j'_a}(l_a\tfrac{1}{2})_{j_a}|(l_al'_a)_K(\tfrac{1}{2}\tfrac{1}{2})_0\right)_K\left((l'_b\tfrac{1}{2})_{j'_b}(l_b\tfrac{1}{2})_{j_b}|(l_bl'_b)_K(\tfrac{1}{2}\tfrac{1}{2})_0\right)_K\\
&\times\frac{2l_a+1}{2K+1}\langle l'_a\ m_a-m'_a-M\ 1/2\ m'_a|j'_a\ m_a-M\rangle\\
&\times\langle l_a\ 0\ 1/2\ m_a|j_a\ m_a\rangle Y^{l'_a}_{m_a-m'_a-M}(\hat{\mathbf{k}}'_a)\mathcal{I}(l_a,l'_a,j_a,j'_a,j'_b,K),
\end{aligned}\tag{6.G.61}$$

J. Bardeen and D. Pines. Electron-phonon interaction in metals. *Phys. Rev.*, 99: 1140, 1955.

G. F. Bertsch, P. F. Bortignon, and R. A. Broglia. Damping of nuclear excitations. *Rev. Mod. Phys.*, 55:287, 1983.

D. R. Bès and R. A. Broglia. Equivalence between Feynman–Goldstone and particle–phonon diagrams for finite many body systems. In G. Alaga, V. Paar, and L. Sips, editors, ~~*Problems of Vibrational Nuclei,*~~ *in Procs. of the topical Conference on Problems of Vibrational Nuclei*, page 1, Amsterdam, 1975. North Holland.

Proceedings of the

D. R. Bès and R. A. Broglia. In A. Bohr and R. Broglia, editors, *International School of Physics "Enrico Fermi" Course LXIX, Elementary Modes of Excitation in Nuclei*, page 55, Amsterdam, 1977. North Holland.

D. R. Bès and J. Kurchan. *The tratment of Collective Coordinates in Many–Body Systems*. World Scientific, Singapore, 1990.

D. R. Bès, G. G. Dussel, R. Broglia, R. Liotta, and B. R. Mottelson. Nuclear field theory as a method of treating the problem of overcompleteness in descriptions involving elementary modes of both quasi-particles and collective type. *Phys. Lett. B*, 52:253, 1974.

D. R. Bès, R. A. Broglia, G. G. Dussel, R. J. Liotta, and R. P. J. Perazzo. On the many-body foundation of the Nuclear Field Theory. *Nucl. Phys. A*, 260:77, 1976a.

D. R. Bès, R. A. Broglia, G. G. Dussel, R. J. Liotta, and H. M. Sofía. The nuclear field treatment of some exactly soluble models. *Nucl. Phys. A*, 260:1, 1976b.

D. R. Bès, R. A. Broglia, G. G. Dussel, R. J. Liotta, and H. M. Sofía. Application of the nuclear field theory to monopole interactions which include all the vertices of a general force. *Nucl. Phys. A*, 260:27, 1976c.

A. Bohr and B. R. Mottelson. *Nuclear Structure, Vol.I.* Benjamin, New York, 1969.

A. Bohr and B. R. Mottelson. *Nuclear Structure, Vol.II.* Benjamin, New York, 1975.

M. Born. Zur Quantenmechanik der Stoßvorgänge. *Zeitschr. f. Phys.*, 37:863, 1926.

P. Bortignon, A. Bracco, and R. Broglia. *Giant Resonances*. Harwood Academic Publishers, Amsterdam, 1998.

P. F. Bortignon and R. A. Broglia. Role of the nuclear surface in a unified description of the damping of single–particle states and giant resonances. *Nucl. Phys. A*, 371:405, 1981.

P. F. Bortignon, R. A. Broglia, and C. H. Dasso. Quenching of the mass operator associated with collective states in many–body systems. *Nuclear Physics A*, 398: 221, 1983.

D. Brink and R. A. Broglia. *Nuclear Superfluidity*. Cambridge University Press, Cambridge, 2005.

D. Brink and G. R. Satchler. *Angular Momentum*. Clarendon Press, 1968.

R. Broglia and A. Winther. *Heavy Ion Reactions*. Westview Press, Cambridge, MA., 2004.

R. Broglia, O. Hansen, and C. Riedel. Two–neutron transfer reactions and the pairing model. *Advances in Nuclear Physics*, 6:287, 1973. URL http://merlino.mi.infn.it/repository/BrogliaHansenRiedel.pdf.

R. Broglia, G. Coló, G. Onida, and H. Roman. *Solid State Physics of Finite Systems: metal clusters, fullerenes, atomic wires*. Springer Verlag, Berlin, Heidelberg, 2004.

R. A. Broglia, B. R. Mottelson, D. R. Bès, R. Liotta, and H. M. Sofía. Treatment of the spurious state in Nuclear Field Theory. *Physics Letters B*, 64:29, 1976.

P. F. Bortignon, R. A. Broglia and C. H. Dasso,
C. Mahaux, ~~et al~~. Dynamics of the shell model. *Physics Reports*, 120:1–274, 1985.

W. R. Cobb and D. B. Guthe. Angular distribution of protons from the $^{44}Ca(d,p)^{45}Ca$ reaction. *Phys. Rev.*, 107:181, 1957.

W. H. Dickhoff and C. Barbieri. Self–consistent green's function method for nuclei and nuclear matter. *Progress in Particle and Nuclear Physics*, 52:377, 2004.

T. Duguet and G. Hagen. *Ab initio* approach to effective single-particle energies in doubly closed shell nuclei. *Phys. Rev. C*, 85:034330, 2012.

A. R. Edmonds. *Angular momentum in quantum mechanics*. Princeton University Press, 1960.

all the authors
F. Barranco ~~et al.~~ The halo of the exotic nucleus $^{11}Li$: a single Cooper pair. *Europ. Phys. J. A*, 11:385, 2001.

R. Feynman. *Theory of fundamental processes*. Benjamin, Reading, Mass., 1975.

H. Frohlich. Interaction of electrons with lattice vibrations. *Procs. Royal Soc.*, 215:291, 1952. Nucl. Phys.

I. Hamamoto. Single-particle components of particle-vibrational states in the nuclei $^{209}Pb$, $^{209}Bi$, $^{207}Pb$ and $^{207}Tl$. *Nuclear Physics A*, 141:1, 1970.

I. Tanihata et al. Measurement of the two-halo neutron transfer reaction $^{1}H(^{11}Li,^{9}Li)^{3}H$ at 3A MeV. *Phys. Rev. Lett.*, 100:192502, 2008.

R.A. Broglia, D.R. Bès and R. Liotta




B. K. Jenning. Non observability of spectroscopic factors. *arXiv: 1102.3721ve [nucl-th]*, 2011.

A. Migdal. Interaction between electrons and lattice vibrations in a normal metal. *Soviet Physics JETP*, 7:996, 1958.

B. R. Mottelson. *Elementary Modes of Excitation in Nuclei, Le Prix Nobel en 1975*. Imprimerie Royale Norstedts Tryckeri, Stockholm, 1976. p. 80.

P. F. Bortignon ~~et al~~. Nuclear field theory. *Physics Reports*, 30:305, 1977.

W. Pauli. *Exclusion principle and quantum mechanics, Nobel Lecture 1945*. Editions du Griffon, Neuchâtel, Switzerland, 1947.

G. Potel, F. Barranco, E. Vigezzi, and R. A. Broglia. Evidence for phonon mediated pairing interaction in the halo of the nucleus $^{11}$Li. *Phys. Rev. Lett.*, 105:172502, 2010.

G. Potel, A. Idini, F. Barranco, E. Vigezzi, and R. A. Broglia. Cooper pair transfer in nuclei. *Rep. Prog. Phys.*, 76:106301, 2013.

G. Satchler. *Introduction to Nuclear Reactions*. Mc Millan, New York, 1980.

J. Vaagen, B. Nilsson, J. Bang, and R. Ibarra. One– and two–nucleon overlaps generated by a Sturmian method. *Nuclear Physics A*, 319:143, 1979.